

Super-Planckian Electron Cooling in a van der Waals Stack

Alessandro Principi,¹ Mark B. Lundberg,² Niels C. H. Hesp,² Klaas-Jan Tielrooij,²
Frank H. L. Koppens,^{2,3} and Marco Polini⁴

¹*Radboud University, Institute for Molecules and Materials, NL-6525 AJ Nijmegen, The Netherlands*

²*ICFO-Institut de Ciències Fotòniques, The Barcelona Institute of Science
and Technology, 08860 Castelldefels (Barcelona), Spain*

³*ICREA-Institució Catalana de Recerca i Estudis Avançats, Barcelona, Spain*

⁴*Istituto Italiano di Tecnologia, Graphene Labs, Via Morego 30, I-16163 Genova, Italy*

(Received 23 August 2016; published 24 March 2017)

Radiative heat transfer (RHT) between macroscopic bodies at separations that are much smaller than the thermal wavelength is ruled by evanescent electromagnetic modes and can be orders of magnitude more efficient than its far-field counterpart, which is described by the Stefan-Boltzmann law. In this Letter, we present a microscopic theory of RHT in van der Waals stacks comprising graphene and a natural hyperbolic material, i.e., hexagonal boron nitride (hBN). We demonstrate that RHT between hot carriers in graphene and hyperbolic phonon polaritons in hBN is extremely efficient at room temperature, leading to picosecond time scales for the carrier cooling dynamics.

DOI: 10.1103/PhysRevLett.118.126804

Introduction.—The cooling of hot carriers in a crystal typically proceeds via energy transfer to phonons [1]. In graphene, ultralong cooling times, of the order of nanoseconds, have been theoretically predicted [2,3]. Such slow cooling dynamics is due to energy transfer to graphene acoustic phonons via collisions that conserve momentum. These are greatly inefficient because of the large mismatch between the electron and acoustic-phonon momentum. If realized experimentally, the slow intrinsic cooling time would imply notable figures of merit for graphene-based photodetectors [4]. Unfortunately, the cooling dynamics in “first-generation” graphene samples [5], deposited on SiO₂, is believed to be dominated by far more efficient disorder-assisted collisions between electrons and graphene acoustic phonons [6–9]. According to theory [8,9], such “super-collisions” are due to short-range disorder.

In this respect, a natural question arises: What is the fate of the temperature dynamics of hot carriers in “second-generation” samples [10], where graphene is encapsulated between hexagonal boron nitride (hBN) crystals [11–16]? On the one hand, these samples have shown nearly ideal transport characteristics [11–16], whereby electron-acoustic phonon scattering [17,18] fully determines dc transport times at room temperature, at least for sufficiently large carrier densities. On the other hand, hBN crystal slabs are known to support low-loss standing Fabry-Pérot modes between the reflecting top and bottom interfaces [19–21]. These modes occur because hBN is a uniaxial crystal with intrinsic *hyperbolic* character [22], i.e., with in- (ϵ_x) and out-of-plane (ϵ_z) components of the dielectric tensor $\hat{\epsilon}$ having opposite signs in the “reststrahlen” frequency bands.

An important question rises if hot carriers in graphene can transfer their energy to the phonon polaritons in hBN.

This radiative heat transfer (RHT) would then significantly affect the carrier cooling dynamics. In this Letter, we answer this question affirmatively.

RHT between macroscopic bodies has been studied since the early days of 1900, when Planck explained the black-body radiation spectrum. In the regime $\delta \gg d_T$ (far-field regime), where δ is the separation between two bodies and $d_T = \hbar c / (k_B T)$ is the thermal wavelength, RHT is due to traveling electromagnetic (EM) waves and is controlled by the Stefan-Boltzmann law. On the contrary, in the limit $\delta \ll d_T$ (near-field regime) RHT is dominated by evanescent modes of the EM field and power transfer can greatly exceed the black-body limit (“super-Planckian” thermal emission). Anomalous RHT between closely spaced bodies was first studied experimentally by Hargreaves [23]. This pioneering work motivated the introduction of a general theoretical formalism [24], which was based on the theory of fluctuating electrodynamics [25–27]. Near-field thermal coupling has been intensively studied in the past both experimentally [28–33] and theoretically [34–41].

Electron temperature dynamics and hyperbolic phonon polaritons.—In this work we consider the encapsulated graphene heterostructure depicted in Fig. 1. A single layer of graphene is embedded between two hyperbolic dielectric slabs of thickness d and d' , located below and above the graphene sheet, respectively. We therefore set the spacing $\delta = 0$. We present a theoretical study of the temperature dynamics of hot electrons in graphene—behaving as a two-dimensional (2D) gas of hot massless Dirac fermions (MDFs) [42]—due to the near-field radiative coupling to phonon polaritons in the nearby dielectrics, kept at the equilibrium temperature T_L . While our theory is completely general, explicit numerical results will be reported for the case of hBN.

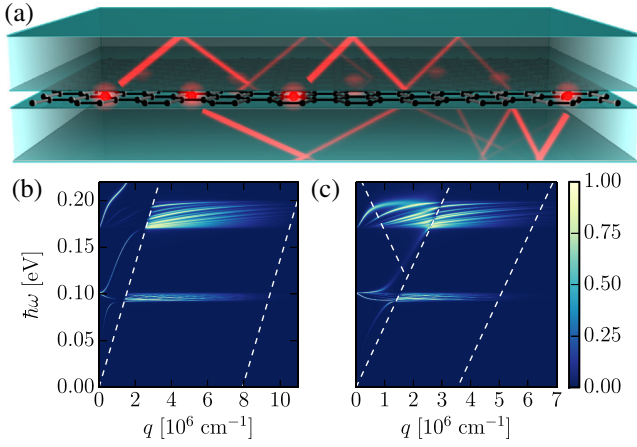


FIG. 1. (a) A schematic view of the physical system: hot carriers in graphene (red spherical balls) efficiently radiate energy into phonon-polariton modes in nearby hyperbolic crystal slabs (semitransparent green parallelepipeds). (b),(c) Color plots of the dimensionless function $\mathcal{Z}(q, \omega)$ in Eq. (5) for an electron temperature $T_e = 300$ K and top (bottom) hBN thickness $d' = 9$ nm ($d = 27$ nm). All other parameters are reported in Ref. [43]. (b) $n = 5.0 \times 10^{12}$ cm $^{-2}$. (c) $n = 1.0 \times 10^{12}$ cm $^{-2}$. Dashed lines indicate the edges of the graphene particle-hole continua [42]. In panel (b), the bottom edge of the interband continuum is not present since it occurs well above the hBN reststrahlen bands for $n = 5 \times 10^{12}$ cm $^{-2}$. The quantity $\mathcal{Z}(q, \omega)$ is maximum at the location of the poles of the dressed Coulomb interaction $V_{q,\omega}$ (standing hBN phonon polaritons [19,20]) and at the zeros of the dynamical dielectric function $\epsilon(q, \omega)$ (plasmon-phonon polaritons [15,21]).

The temperature T_e of hot carriers in graphene satisfies the following differential equation:

$$\partial_t T_e = -\frac{T_e - T_L}{\tau(T_e, T_L)}, \quad (1)$$

where $\tau(T_e, T_L) \equiv C_n(T_e - T_L)/\mathcal{Q}$. Here \mathcal{Q} is the rate of heat transfer between hot electrons and phonon polaritons while C_n is the electronic heat capacity at a constant density n . In the limit $\Delta T \equiv T_e - T_L \rightarrow 0$, one can expand \mathcal{Q} for small values of ΔT and the ratio $(T_e - T_L)/\mathcal{Q}$ does *not* depend on T_e , i.e.,

$$\tau^* \equiv \lim_{\Delta T \rightarrow 0} \tau(T_e, T_L) = \left(\frac{1}{C_n} \frac{\partial \mathcal{Q}}{\partial T_e} \Big|_{T_e=T_L} \right)^{-1}. \quad (2)$$

In this case, Eq. (1) implies a simple exponential decay in time, $T_e(t) = T_e(0) \exp(-t/\tau^*)$ and τ^* acquires the physical meaning of a *cooling time scale*. As we demonstrate below, for the problem at hand we find

$$C_n = \sum_{k,\lambda} \left(-\frac{\partial f_{k,\lambda}}{\partial \epsilon_{k,\lambda}} \right) \xi_{k,\lambda}(T_e) \left(\frac{\xi_{k,\lambda}(T_e)}{T_e} + \frac{\partial \mu(T_e)}{\partial T_e} \right), \quad (3)$$

$$\mathcal{Q} = \frac{\hbar}{4} \int \frac{d^2 \mathbf{q}}{(2\pi)^2} \int_{-\infty}^{\infty} \frac{d\omega}{\pi} \omega [n_B(\omega_e) - n_B(\omega_L)] \mathcal{Z}(q, \omega), \quad (4)$$

and

$$\mathcal{Z}(q, \omega) \equiv 4 \frac{\Im[V_{q,\omega}] \Im[\chi_{nn}^{(0)}(q, \omega)]}{|\epsilon(q, \omega)|^2}. \quad (5)$$

Here, $f_{k,\lambda} \equiv n_F[\xi_{k,\lambda}(T_e)/(k_B T_e)]$, $n_{F/B}(x) = (e^x \pm 1)^{-1}$ is the Fermi-Dirac-Bose-Einstein distribution function, $\omega_{e,L} \equiv \hbar\omega/(k_B T_{e,L})$, $\xi_{k,\lambda}(T_e) \equiv \epsilon_{k,\lambda} - \mu(T_e)$, and $\epsilon_{k,\lambda} = \lambda \hbar v_F k$ is the electronic energy— $\lambda = +1$ ($\lambda = -1$) corresponding to conduction- (valance-)band states and $v_F \sim 10^6$ m/s is the Fermi velocity in graphene. The chemical potential $\mu = \mu(T_e)$ is obtained by requiring the charge density to be time independent and equal to the initial electronic charge $-en$ ($-e$ is the electron charge).

In Eq. (5), $\epsilon(q, \omega) = 1 - V_{q,\omega} \chi_{nn}^{(0)}(q, \omega)$ is the dynamical screening function [21] in the random phase approximation (RPA) [47], with $\chi_{nn}^{(0)}(q, \omega)$ the density-density response function of a 2D system of noninteracting MDFs [48]. Finally, $V_{q,\omega}$ is the instantaneous Coulomb propagator dressed by the presence of the surrounding hyperbolic dielectrics. Its frequency dependence stems from the frequency dependence of the in-plane and out-of-plane permittivities $\epsilon_x(\omega)$ and $\epsilon_z(\omega)$. Explicit expressions for $V_{q,\omega}$, $\epsilon_x(\omega)$ and $\epsilon_z(\omega)$ are reported in Ref. [43]. Poles of the dressed Coulomb interaction $V_{q,\omega}$ yield the dispersion relation of standing phonon-polariton modes in the hyperbolic dielectrics [21].

The hyperbolic nature of hBN sets an extremely efficient intrinsic pathway for the dissipation of heat stored by graphene carriers, yielding cooling times $\tau^* \sim 1$ –10 ps. Cooling into nonhyperbolic polar substrates has been studied, e.g., in Ref. [49]. Below, we set $\hbar = k_B = 1$, unless explicitly stated otherwise.

Boltzmann-transport theory of RHT.—We now demonstrate Eqs. (1), (3), (4), and (5). We start from the semiclassical Boltzmann equation [2,3,8,9] $\partial_t f_{k,\lambda} = -\mathcal{I}_{k,\lambda}$ for the electron distribution function $f_{k,\lambda}$. Here,

$$\mathcal{I}_{k,\lambda} = \sum_{k',\lambda'} \left[f_{k,\lambda} (1 - f_{k',\lambda'}) W_{k,\lambda}^{k',\lambda'} - f_{k',\lambda'} (1 - f_{k,\lambda}) W_{k',\lambda'}^{k,\lambda} \right] \quad (6)$$

is the collision integral, while

$$W_{k,\lambda}^{k',\lambda'} = 2\pi \sum_{q,\nu} |U_{k,q}^{\lambda,\lambda',\nu}|^2 [(n_{q,\nu} + 1) \delta(\Delta\epsilon - \omega_{q,\nu}) \times \delta(\mathbf{k} - \mathbf{k}' - \mathbf{q}) + n_{q,\nu} \delta(\Delta\epsilon + \omega_{q,\nu}) \delta(\mathbf{k} - \mathbf{k}' + \mathbf{q})] \quad (7)$$

is the transition probability. In Eq. (7), $n_{q,\nu}$ is the phonon-polariton distribution function and $\Delta\epsilon = \epsilon_{k,\lambda} - \epsilon_{k',\lambda'}$ the

electronic transition energy. The matrix element of the electron-phonon-polariton interaction, $U_{\mathbf{k},\mathbf{q}}^{\lambda,\lambda',\nu}$, is derived below and contains all the information about the hyperbolic character of the dielectrics.

Multiplying both members of the Boltzmann equation by $\varepsilon_{\mathbf{k},\lambda} - \mu$ and summing over \mathbf{k} , λ we find an equation of motion for the energy density \mathcal{E} : $\partial_t \mathcal{E} = -\tilde{\mathcal{Q}}$, where the energy transfer rate is $\tilde{\mathcal{Q}} = \sum_{\mathbf{k},\lambda} (\varepsilon_{\mathbf{k},\lambda} - \mu) \mathcal{I}_{\mathbf{k},\lambda}$. The left-hand side of this equation can be expressed in terms of the electronic temperature provided that we introduce the heat capacity, i.e., $\partial_t \mathcal{E} = C_n \partial_t T_e$. We now need to work on its right-hand side. To this end, we need to derive the electron-phonon-polariton interaction, $U_{\mathbf{k},\mathbf{q}}^{\lambda,\lambda',\nu}$.

Electron-photon coupling and the hBN-dressed photon propagator.—RHT occurs because of the coupling between hot carriers in graphene and the surrounding three-dimensional (3D) EM field. This coupling is described by the usual light-matter interaction Hamiltonian

$$\mathcal{H}_{\text{ep}} = \frac{e}{cV} \sum_{\mathbf{q}, q_z, \nu} \mathbf{j}_{-\mathbf{q}} \cdot \mathbf{A}_{\mathbf{q}, q_z, \nu}(t), \quad (8)$$

where c is the speed of light in vacuum, V is the 3D quantization volume, $\nu = \text{TM}, \text{TE}$ is the polarization of the EM field, $\mathbf{j}_{\mathbf{q}} = \sum_{\mathbf{k}, \lambda, \lambda'} c_{\mathbf{k}-\mathbf{q}, \lambda}^\dagger \mathbf{J}_{\mathbf{k}-\mathbf{q}, \lambda; \mathbf{k}, \lambda'} c_{\mathbf{k}, \lambda}$ is the MDF particle current operator [42], and $\mathbf{A}_{\mathbf{q}, q_z, \nu}(t)$ are the Fourier components of the EM vector potential (\mathbf{q} is a 2D vector in the graphene plane). Here, $c_{\mathbf{k}, \lambda}^\dagger$ ($c_{\mathbf{k}, \lambda}$) creates (destroys) an electron with momentum \mathbf{k} in band $\lambda = \pm$, and $\mathbf{J}_{\mathbf{k}, \lambda; \mathbf{k}', \lambda'}$ are the matrix elements of the current operator in the band representation [43]. Note that the current operator $\mathbf{j}_{\mathbf{q}}$ (photon field $\mathbf{A}_{\mathbf{q}, q_z, \nu}$) in Eq. (8) is represented by a 2D (3D) vector.

The corresponding 3D photon propagator $G_{\nu, \alpha\beta}^{\text{3D}}(\mathbf{q}, q_z, t) \equiv -ie^2 \langle T A_{\mathbf{q}, q_z, \nu, \alpha}(t) A_{\mathbf{q}, q_z, \nu, \beta}^\dagger \rangle / c^2$ and its Fourier transform $G_{\nu, \alpha\beta}^{\text{3D}}(\mathbf{q}, q_z, \omega)$ contain all the necessary information. Here, “ T ” denotes the time-ordering operator, $\alpha, \beta = x, y, z$ are Cartesian indices, and $\langle \dots \rangle$ denotes an average over the thermal ensemble.

The photon propagator is substantially altered by the phonons in the nearby hyperbolic crystals. This “dressing” can be easily captured analytically in the nonretarded limit, in which the 3D dressed propagator $G_{\nu, \alpha\beta}^{\text{3D}}(\mathbf{q}, q_z, t)$ can be calculated from the knowledge of the 3D instantaneous Coulomb propagator. The latter, in turn, can be calculated by utilizing a straightforward electrostatic approach [21]. The required 2D propagator is obtained integrating over q_z . The end result is [43] $\text{Im}[G_{\nu, \alpha\beta}^{\text{2D}}(\mathbf{q}, \omega)] = q_\alpha q_\beta \Im m[V_{\mathbf{q}, \omega}] / \omega^2$, if $\nu = \text{TM}$, and zero otherwise. The calculation of $\text{Im}[G_{\nu, \alpha\beta}^{\text{2D}}(\mathbf{q}, \omega)]$ allows us to calculate how phonon polaritons dress the squared matrix element of the light-matter interaction [43]

$$|U_{\mathbf{k}, \mathbf{q}}^{\lambda, \lambda', \nu}|^2 = -J_{\mathbf{k}, \lambda; \mathbf{k}_+, \lambda'}^{(\alpha)} J_{\mathbf{k}_+, \lambda'; \mathbf{k}, \lambda}^{(\beta)} \int_0^\infty \frac{d\omega}{\pi} \text{Im}[G_{\nu, \alpha\beta}^{\text{2D}}(\mathbf{q}, \omega)]. \quad (9)$$

Here $\mathbf{k}_+ = \mathbf{k} + \mathbf{q}$. The sum over $\alpha, \beta = x, y$ is understood.

Plugging Eq. (9) into Eqs. (6) and (7) we get the energy transfer rate

$$\tilde{\mathcal{Q}} = - \sum_{\nu} \int \frac{d^2 \mathbf{q}}{(2\pi)^2} \int_{-\infty}^{\infty} \frac{d\omega}{\pi} \omega [n_B(\omega/T_L) - n_B(\omega/T_e)] \times \text{Im}[\chi_{j_\alpha j_\beta}^{(0)}(\mathbf{q}, \omega)] \text{Im}[G_{\nu, \alpha\beta}^{\text{2D}}(\mathbf{q}, \omega)]. \quad (10)$$

Here, $\chi_{j_\alpha j_\beta}^{(0)}(\mathbf{q}, \omega)$ is the current-current response tensor of a 2D system of noninteracting MDFs [50]. To obtain Eq. (10), we assumed that both electrons and phonon polaritons are at equilibrium at the two temperatures T_e (electron temperature) and T_L (lattice temperature), respectively. We finally *bootstrap* Eq. (10) by introducing RPA dynamical screening [47]; i.e., we replace

$$\text{Im}[\chi_{j_\alpha j_\beta}^{(0)}(\mathbf{q}, \omega)] \rightarrow \frac{\text{Im}[\chi_{\text{L}}^{(0)}(\mathbf{q}, \omega)]}{|\varepsilon(\mathbf{q}, \omega)|^2} P_{\alpha\beta}^{\text{L}} + \text{Im}[\chi_{\text{T}}^{(0)}(\mathbf{q}, \omega)] P_{\alpha\beta}^{\text{T}} \quad (11)$$

where $\chi_{\text{L}}^{(0)}(\mathbf{q}, \omega)$ and $\chi_{\text{T}}^{(0)}(\mathbf{q}, \omega)$ are the longitudinal and transverse current-current response functions, while $P_{\alpha\beta}^{\text{L}} = q_\alpha q_\beta / q^2$ and $P_{\alpha\beta}^{\text{T}} = \delta_{\alpha\beta} - P_{\alpha\beta}^{\text{L}}$. Using Eq. (11) in Eq. (10) and the identity $\chi_{nn}^{(0)} = q^2 \chi_{\text{L}}^{(0)} / \omega^2$ [47], and restoring \hbar and k_B , we finally find the desired Eq. (4). The transverse current-current response function $\chi_{\text{T}}^{(0)}(\mathbf{q}, \omega)$ in Eq. (11) drops out of Eq. (4) since $\text{Im}[G_{\nu, \alpha\beta}^{\text{2D}}(\mathbf{q}, \omega)]$ is purely longitudinal. Equations (4) and (5) can also be obtained from fluctuating electrodynamics [43].

Results.—A color plot of $\mathcal{Z}(\mathbf{q}, \omega)$ for typical values of microscopic parameters is reported in Fig. 1. We note that $\mathcal{Z}(\mathbf{q}, \omega)$ is real, dimensionless, and bounded, i.e., $0 \leq \mathcal{Z}(\mathbf{q}, \omega) \leq 1$. The super-Planckian nature of the energy transfer rate in Eq. (4) stems from contributions to the integral coming from phonon-polariton modes with $q \gg \omega/c$, the only natural short-wavelength cutoff ($\sim k_F$) for the integral being provided by $\text{Im}[\chi_{nn}^{(0)}(\mathbf{q}, \omega)]$.

Numerical results for the cooling time τ^* in Eq. (2) are shown in Figs. 2 and 3. In particular, in Fig. 2(a) we plot τ^* as a function of carrier density n , for different values of the electron temperature $T_e = T_L$, while in Fig. 2(b) we plot τ^* as a function of T_e , for different values of n . For most values of the electron density away from the $n = 0$ charge-neutrality point (CNP), τ^* shows a weak dependence on n , because of a cancellation that we now proceed to discuss. Because the integrand in Eq. (4) is proportional to $\text{Im}[\chi_{nn}^{(0)}(\mathbf{q}, \omega)]$, we can separate out contributions to \mathcal{Q} that are due to intraband (i.e., $\omega < v_F q$) and interband electronic excitations [i.e., $\omega > \max(v_F q, 2\varepsilon_F / \hbar - v_F q)$]. There is also a contribution due to plasmon-phonon polaritons (zeros of $\varepsilon(\mathbf{q}, \omega)$, Ref. [21]), which we define by

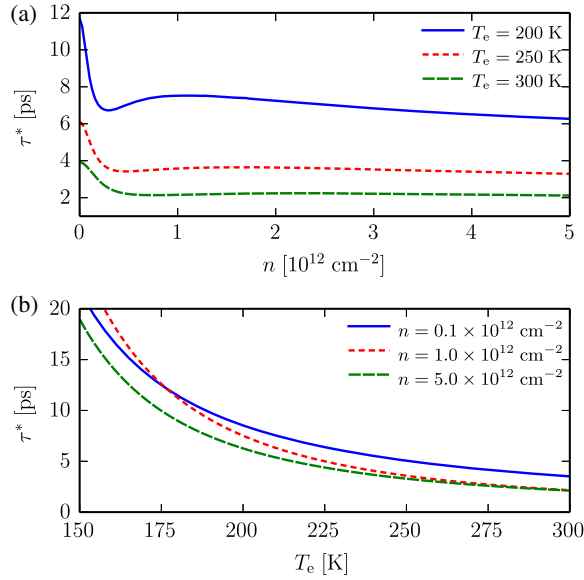


FIG. 2. (a) The cooling time τ^* (2) as a function of the electron density n , for different values of the electron temperature T_e . (b) The cooling time τ^* as a function of T_e for different values of n .

considering contributions to the frequency integral in Eq. (4) coming from the $T = 0$ Pauli-blocking gap, i.e., $v_F q < \omega < 2\varepsilon_F/\hbar - v_F q$. These three contributions to the cooling rate $1/\tau^*$ are shown in Fig. 3(a). We clearly see that the intraband contribution is dominant for most values of the carrier density, with the exclusion of the low-density regime, where intra- and interband contributions become comparable in magnitude. Note also that the increase with n of the intraband contribution is nearly exactly cancelled by a decrease with n of the interband contribution. This explains the weak dependence of τ^* on n away from the CNP displayed in Figs. 2(a). The contribution due to the plasmon-phonon polariton branch is negligible.

The role of the hyperbolic character of the dielectric slabs surrounding graphene is significant. We reveal this in Fig. 3(b), which shows the cooling efficiency of the process investigated in this work by comparing RHT into hyperbolic phonon polaritons (solid line) to RHT into non-hyperbolic phonon polaritons (grey-shaded area). The latter is calculated by using Eqs. (4), (5), and (2) one time with $\varepsilon_x(\omega) \rightarrow \varepsilon_z(\omega)$ in the equation for $V_{q,\omega}$, and one time with $\varepsilon_z(\omega) \rightarrow \varepsilon_x(\omega)$. These replacements make sure that the crystal slabs surrounding graphene are nonhyperbolic. We clearly see that RHT into standing hyperbolic phonon-polariton modes is far more efficient.

Before concluding, we would like to discuss temperature dynamics in the overheating $T_e \gg T_L$ regime. As we have seen above, for $T_e \approx T_L$ the function $T_e(t)$ is an exponential with time scale τ^* . This exponentially fast equilibration does not occur, however, for $T_e \gg T_L$. In this case, the temperature dynamics $T_e(t)$ can be found by solving Eq. (1) with an initial condition, $T_e(0)$. In Fig. 4(a) we show that the solution

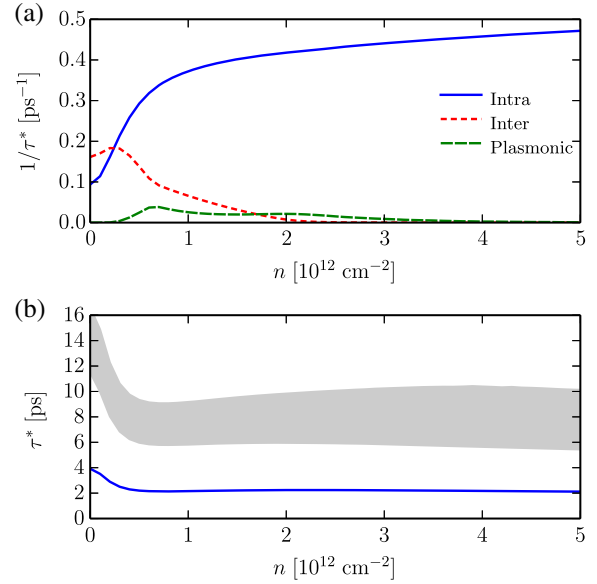


FIG. 3. (a) Intraband (solid line), interband (short-dashed line), and plasmon-phonon polariton (long-dashed line) contributions to the cooling rate $1/\tau^*$. The separate contributions to $1/\tau^*$ are plotted as functions of electron density. (b) A comparison between cooling times for RHT into hBN (blue line) and a nonhyperbolic crystal with identical phonon properties (grey-shaded area). RHT into hyperbolic phonon polaritons is clearly much more efficient. All data for τ^* have been calculated by setting $T_e = T_L = 300$ K.

of this equation for $T_e(0) = 1000$ K $\gg T_L = 1$ K (solid line) displays a slow decay. Note that, even after 30 ps, the electrons are not equilibrated with the lattice. On the contrary, for $T_L = 300$ K, the dynamics is exponential (dashed line).

In summary, we have presented a theory of near-field thermal radiation transfer between hot carriers in graphene and hyperbolic phonon polaritons in nearby dielectric slabs. Our theory is relevant for understanding the cooling dynamics in ultraclean hBN-encapsulated samples [10–16], where

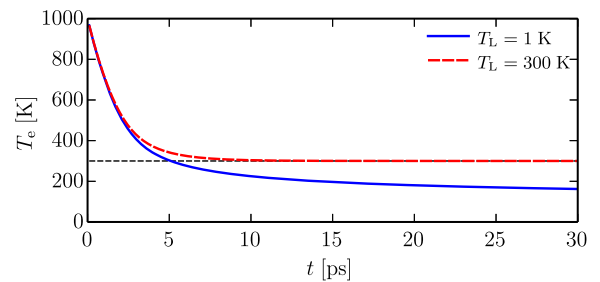


FIG. 4. Cooling dynamics into hyperbolic phonon polaritons. We present typical results of the numerical solution of the complete heat equation, Eq. (1), where we retained the full dependence of $\tau(T_e, T_L)$ on $T_e(t)$. These data have been obtained by setting $T_e(0) = 1000$ K, $T_L = 1$ K (solid line) and $T_L = 300$ K (dashed line), and $n = 10^{12}$ cm $^{-2}$. We clearly see that, for $T_L = 300$ K, equilibration with the lattice occurs exponentially fast.

extrinsic mechanisms [6,7] due to disorder are expected not to be at play. We have discovered that hyperbolic phonon polaritons are extremely efficient heat sinks for hot carriers in graphene at room temperature, leading to picosecond time scales for the carrier cooling dynamics in graphene. Within the realm of high-quality samples, this understanding offers a pathway to tuning cooling times by the hBN thickness, which controls the standing phonon polaritons shown in Fig. 1. Thinner hBN slabs tend to lengthen the cooling time, which is a relevant direction for greatly improving the sensitivity of photodetectors [4].

This work was supported by the European Union's Horizon 2020 research and innovation programme under grant agreement No. 696656 “Graphene flagship,” Fondazione Istituto Italiano di Tecnologia, the Spanish Ministry of Economy and Competitiveness through the “Severo Ochoa” Programme for Centres of Excellence in R&D (SEV-2015-0522), Fundacio Cellex Barcelona, the Mineco Grants Ramón y Cajal (No. RYC-2012-12281), Plan Nacional (No. FIS2013-47161-P), a “Young Investigator Grant” (No. FIS2014-59639-JIN), the Government of Catalonia through the SGR Grant (No. 2014-SGR-1535), the ERC StG “CarbonLight” (307806), and the ERC AdG “FEMTO/NANO” (338957), CERCA Programme/ Generalitat de Catalunya. M. B. L. wishes to thank M. Jablan for useful conversations. M. P. is extremely grateful for the financial support granted by ICFO during a visit where this work was started.

-
- [1] *Hot Carriers in Semiconductors*, edited by J. Shah and G. J. Iafrate (Academic, London, 1992).
- [2] R. Bistritzer and A. H. MacDonald, *Phys. Rev. Lett.* **102**, 206410 (2009).
- [3] W.-K. Tse and S. Das Sarma, *Phys. Rev. B* **79**, 235406 (2009).
- [4] K. H. L. Koppens, T. Mueller, Ph. Avouris, A. C. Ferrari, M. S. Vitiello, and M. Polini, *Nat. Nanotechnol.* **9**, 780 (2014).
- [5] A. K. Geim and K. S. Novoselov, *Nat. Mater.* **6**, 183 (2007).
- [6] A. C. Betz, S. H. Jhang, E. Pallecchi, R. Ferreira, G. Fève, J.-M. Berroir, and B. Plaçaïs, *Nat. Phys.* **9**, 109 (2012).
- [7] M. W. Graham, S.-F. Shi, D. C. Ralph, J. Park, and P. L. McEuen, *Nat. Phys.* **9**, 103 (2013).
- [8] J. C. W. Song, M. Y. Reizer, and L. S. Levitov, *Phys. Rev. Lett.* **109**, 106602 (2012).
- [9] J. C. W. Song and L. S. Levitov, *J. Phys. Condens. Matter* **27**, 164201 (2015).
- [10] A. K. Geim and I. V. Grigorieva, *Nature (London)* **499**, 419 (2013).
- [11] A. S. Mayorov, R. V. Gorbachev, S. V. Morozov, L. Britnell, R. Jalil, L. A. Ponomarenko, P. Blake, K. S. Novoselov, K. Watanabe, T. Taniguchi, and A. K. Geim, *Nano Lett.* **11**, 2396 (2011).
- [12] A. S. Mayorov, D. C. Elias, I. S. Mukhin, S. V. Morozov, L. A. Ponomarenko, K. S. Novoselov, A. K. Geim, and R. V. Gorbachev, *Nano Lett.* **12**, 4629 (2012).
- [13] L. Wang, I. Meric, P. Y. Huang, Q. Gao, Y. Gao, H. Tran, T. Taniguchi, K. Watanabe, L. M. Campos, D. A. Muller, J. Guo, P. Kim, J. Hone, K. L. Shepard, and C. R. Dean, *Science* **342**, 614 (2013).
- [14] T. Taychatanapat, K. Watanabe, T. Taniguchi, and P. Jarillo-Herrero, *Nat. Phys.* **9**, 225 (2013).
- [15] A. Woessner, M. B. Lundeberg, Y. Gao, A. Principi, P. Alonso-González, M. Carrega, K. Watanabe, T. Taniguchi, G. Vignale, M. Polini, J. Hone, R. Hillenbrand, and F. H. L. Koppens, *Nat. Mater.* **14**, 421 (2015).
- [16] D. Bandurin, I. Torre, R. K. Kumar, M. Ben Shalom, A. Tomadin, A. Principi, G. H. Auton, E. Khestanova, K. S. Novoselov, I. V. Grigorieva, L. A. Ponomarenko, A. K. Geim, and M. Polini, *Science* **351**, 1055 (2016).
- [17] E. H. Hwang and S. Das Sarma, *Phys. Rev. B* **77**, 115449 (2008).
- [18] A. Principi, M. Carrega, M. B. Lundeberg, A. Woessner, F. H. L. Koppens, G. Vignale, and M. Polini, *Phys. Rev. B* **90**, 165408 (2014).
- [19] S. Dai, Z. Fei, Q. Ma, A. S. Rodin, M. Wagner, A. S. McLeod, M. K. Liu, W. Gannett, W. Regan, K. Watanabe, T. Taniguchi, M. Thiemens, G. Dominguez, A. H. Castro Neto, A. Zettl, F. Keilmann, P. Jarillo-Herrero, M. M. Fogler, and D. N. Basov, *Science* **343**, 1125 (2014).
- [20] J. D. Caldwell, A. Kretinin, Y. Chen, V. Giannini, M. M. Fogler, Y. Francescato, C. T. Ellis, J. G. Tischler, C. R. Woods, A. J. Giles, M. Hong, K. Watanabe, T. Taniguchi, S. A. Maier, and K. S. Novoselov, *Nat. Commun.* **5**, 5221 (2014).
- [21] A. Tomadin, A. Principi, J. C. W. Song, L. S. Levitov, and M. Polini, *Phys. Rev. Lett.* **115**, 087401 (2015).
- [22] A. Poddubny, I. Iorsh, P. Belov, and Y. Kivshar, *Nat. Photonics* **7**, 948 (2013).
- [23] C. M. Hargreaves, *Phys. Lett. A* **30**, 491 (1969).
- [24] D. Polder and M. Van Hove, *Phys. Rev. B* **4**, 3303 (1971).
- [25] S. M. Rytov, *Theory of Electric Fluctuations and Thermal Radiation* (Academy of Sciences of USSR, Moscow, 1953).
- [26] E. M. Lifshitz, *ZhETF* **29**, 94 (1955) [*Sov. Phys. JETP* **2**, 73 (1956)].
- [27] I. E. Dzyaloshinskii, E. M. Lifshitz, and L. P. Pitaevskii, *Adv. Phys.* **10**, 165 (1961).
- [28] Y. De Wilde, F. Formanek, R. Carminati, B. Gralak, P.-A. Lemoine, K. Joulain, J.-P. Mulet, Y. Chen, and J.-J. Greffet, *Nature (London)* **444**, 740 (2006).
- [29] S. Shen, A. Narayanaswamy, and G. Chen, *Nano Lett.* **9**, 2909 (2009).
- [30] E. Rousseau, A. Siria, G. Jourdan, S. Volz, F. Comin, J. Chevrier, and J.-J. Greffet, *Nat. Photonics* **3**, 514 (2009).
- [31] R. S. Ottens, V. Quetschke, S. Wise, A. A. Alemi, R. Lundock, G. Mueller, D. H. Reitze, D. B. Tanner, and B. F. Whiting, *Phys. Rev. Lett.* **107**, 014301 (2011).
- [32] A. C. Jones and M. B. Raschke, *Nano. Lett.* **12**, 1475 (2012).
- [33] K. Kim, B. Song, V. Fernández-Hurtado, W. Lee, W. Jeong, L. Cui, D. Thompson, J. Feist, M. T. Homer Reid, F. J. García-Vidal, J. C. Cuevas, E. Meyhofer, and P. Reddy, *Nature (London)* **528**, 387 (2015).
- [34] J. B. Pendry, *J. Phys. Condens. Matter* **11**, 6621 (1999).

- [35] A. I. Volokitin and B. N. J. Persson, *Phys. Rev. B* **63**, 205404 (2001).
- [36] P. Ben-Abdallah and K. Joulain, *Phys. Rev. B* **82**, 121419 (2010).
- [37] Y. Guo, C. L. Cortes, S. Molesky, and Z. Jacob, *Appl. Phys. Lett.* **101**, 131106 (2012).
- [38] R. Messina, M. Tschikin, S.-A. Biehs, and P. Ben-Abdallah, *Phys. Rev. B* **88**, 104307 (2013).
- [39] P. Ben-Abdallah and S.-A. Biehs, *Phys. Rev. Lett.* **112**, 044301 (2014).
- [40] X. L. Liu, R. Z. Zhang, and Z. M. Zhang, *ACS Photonics* **1**, 785 (2014).
- [41] O. D. Miller, S. G. Johnson, and A. W. Rodriguez, *Phys. Rev. Lett.* **115**, 204302 (2015).
- [42] V. N. Kotov, B. Uchoa, V. M. Pereira, F. Guinea, and A. H. Castro Neto, *Rev. Mod. Phys.* **84**, 1067 (2012).
- [43] See Supplemental Material at <http://link.aps.org/supplemental/10.1103/PhysRevLett.118.126804> for the two-dimensional instantaneous Coulomb propagator as dressed by hBN phonon polaritons. We also report explicit expressions for the hBN permittivities and list all the geometric parameters of the heterostructure that were used for carrying out the calculations reported in the main text. Furthermore, we show a calculation of the cooling time of a graphene sheet placed on a silicon dioxide substrate. Finally, we derive the central formulas of the main text with a fluctuation-electrodynamic approach, which includes Refs. [44–46].
- [44] M. K. Gunde, *Physica (Amsterdam)* **292B**, 286 (2000).
- [45] R. Twiss, *J. Appl. Phys.* **26**, 599 (1955). R. Kubo, *J. Phys. Soc. Jpn.* **12**, 570 (1957). S. M. Rytov, Y. A. Kravtsov, and V. I. Tatarskii, *Elements of Random Fields*, Principles of Statistical Radiophysics Vol. 3 (Springer, Berlin, 1989).
- [46] S. Teitler and B. W. Hennis, *J. Opt. Soc. Am.* **60**, 830 (1970).
- [47] G. F. Giuliani and G. Vignale, *Quantum Theory of the Electron Liquid* (Cambridge University Press, Cambridge, England, 2005).
- [48] B. Wunsch, T. Stauber, F. Sols, and F. Guinea, *New J. Phys.* **8**, 318 (2006); E. H. Hwang and S. Das Sarma, *Phys. Rev. B* **75**, 205418 (2007).
- [49] T. Low, V. Perebeinos, R. Kim, M. Freitag, and Ph. Avouris, *Phys. Rev. B* **86**, 045413 (2012).
- [50] A. Principi, M. Polini, and G. Vignale, *Phys. Rev. B* **80**, 075418 (2009).